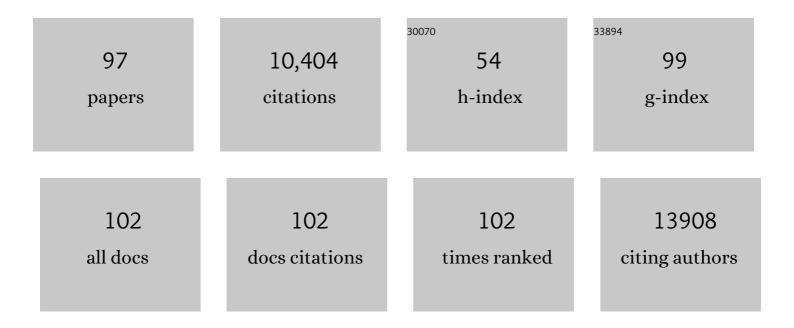
## List of Publications by Year in descending order

Source: https://exaly.com/author-pdf/6014269/publications.pdf Version: 2024-02-01



#	Article	IF	CITATIONS
1	Bimetallic MOF derived nickel nanoclusters supported by nitrogen-doped carbon for efficient electrocatalytic CO2 reduction. Nano Research, 2023, 16, 4546-4553.	10.4	11
2	Super-resolution imaging of photogenerated charges on CdS/g-C <sub>3</sub> N <sub>4</sub> heterojunctions and its correlation with photoactivity. Nanoscale, 2022, 14, 5612-5624.	5.6	10
3	TEMPO-Oxidized Microcrystalline Cellulose for Rapid Adsorption of Ammonium. Industrial & Engineering Chemistry Research, 2022, 61, 7665-7673.	3.7	6
4	Hydrophobic ceramic membranes fabricated via fatty acid chloride modification for solvent resistant membrane distillation (SR-MD). Journal of Membrane Science, 2022, 658, 120715.	8.2	5
5	Elucidating Reaction Pathways of the CO <sub>2</sub> Electroreduction via Tailorable Tortuosities and Oxidation States of Cu Nanostructures. Advanced Functional Materials, 2022, 32, .	14.9	9
6	Flame Synthesized Blue TiO <sub>2â^'</sub> <i><sub>x</sub></i> with Tunable Oxygen Vacancies from Surface to Grain Boundary to Bulk. Small Methods, 2021, 5, e2000928.	8.6	28
7	Novel Nickel-Based Single-Atom Alloy Catalyst for CO <sub>2</sub> Conversion Reactions: Computational Screening and Reaction Mechanism Analysis. Journal of Physical Chemistry C, 2021, 125, 4041-4055.	3.1	14
8	Investigating CO <sub>2</sub> Methanation on Ni and Ru: DFT Assisted Microkinetic Analysis. ChemCatChem, 2021, 13, 2420-2433.	3.7	19
9	Single-Ni Sites Embedded in Multilayer Nitrogen-Doped Graphene Derived from Amino-Functionalized MOF for Highly Selective CO <sub>2</sub> Electroreduction. ACS Sustainable Chemistry and Engineering, 2021, 9, 3792-3801.	6.7	24
10	Effective separation of water-DMSO through solvent resistant membrane distillation (SR-MD). Water Research, 2021, 197, 117103.	11.3	21
11	In situ formation of amorphous Fe-based bimetallic hydroxides from metal-organic frameworks as efficient oxygen evolution catalysts. Chinese Journal of Catalysis, 2021, 42, 1370-1378.	14.0	37
12	Manipulating Intermediates at the Au–TiO <sub>2</sub> Interface over InP Nanopillar Array for Photoelectrochemical CO <sub>2</sub> Reduction. ACS Catalysis, 2021, 11, 11416-11428.	11.2	48
13	TiO2 with controllable oxygen vacancies for efficient isopropanol degradation: photoactivity and reaction mechanism. Catalysis Science and Technology, 2021, 11, 4060-4071.	4.1	9
14	Wetting-regulated gas-involving (photo)electrocatalysis: biomimetics in energy conversion. Chemical Society Reviews, 2021, 50, 10674-10699.	38.1	63
15	Rational Synthesis of Amorphous Ironâ€Nickel Phosphonates for Highly Efficient Photocatalytic Water Oxidation with Almost 100 % Yield. Angewandte Chemie - International Edition, 2020, 59, 1171-1175.	13.8	32
16	Rational Synthesis of Amorphous Ironâ€Nickel Phosphonates for Highly Efficient Photocatalytic Water Oxidation with Almost 100 % Yield. Angewandte Chemie, 2020, 132, 1187-1191.	2.0	4
17	Isolated Ni single atoms in nitrogen doped ultrathin porous carbon templated from porous g-C3N4 for high-performance CO2 reduction. Nano Energy, 2020, 77, 105158.	16.0	83
18	Development of metal sulfide–based photocatalysts for hydrogen evolution under visible light. , 2020. , 369-384.		4

<sup>18</sup> 2020, , 369-384.

#	Article	IF	CITATIONS
19	Anchoring Active Pt <sup>2+</sup> /Pt <sup>0</sup> Hybrid Nanodots on gâ€C <sub>3</sub> N <sub>4</sub> Nitrogen Vacancies for Photocatalytic H <sub>2</sub> Evolution. ChemSusChem, 2019, 12, 2029-2034.	6.8	54
20	Research advances towards large-scale solar hydrogen production from water. EnergyChem, 2019, 1, 100014.	19.1	130
21	Hierarchically Structured Janus Membrane Surfaces for Enhanced Membrane Distillation Performance. ACS Applied Materials & Interfaces, 2019, 11, 25524-25534.	8.0	97
22	Isolated Squareâ€Planar Copper Center in Boron Imidazolate Nanocages for Photocatalytic Reduction of CO <sub>2</sub> to CO. Angewandte Chemie, 2019, 131, 11878-11882.	2.0	32
23	Magnetic Hollow Spheres Assembled from Graphene-Encapsulated Nickel Nanoparticles for Efficient Photocatalytic CO <sub>2</sub> Reduction. ACS Applied Energy Materials, 2019, 2, 7670-7678.	5.1	78
24	MOF-derived hierarchical hollow spheres composed of carbon-confined Ni nanoparticles for efficient CO <sub>2</sub> methanation. Catalysis Science and Technology, 2019, 9, 731-738.	4.1	87
25	Isolated Squareâ€Planar Copper Center in Boron Imidazolate Nanocages for Photocatalytic Reduction of CO <sub>2</sub> to CO. Angewandte Chemie - International Edition, 2019, 58, 11752-11756.	13.8	194
26	Bifunctional metal–organic frameworks toward photocatalytic CO2 reduction by post-synthetic ligand exchange. Rare Metals, 2019, 38, 413-419.	7.1	68
27	New Family of Plasmonic Photocatalysts without Noble Metals. Chemistry of Materials, 2019, 31, 2320-2327.	6.7	25
28	Emerging applications of nanocatalysts synthesized by flame aerosol processes. Current Opinion in Chemical Engineering, 2018, 20, 39-49.	7.8	24
29	Co <sub>3</sub> O <sub>4</sub> and Fe <sub><i>x</i></sub> Co <sub>3–<i>x</i></sub> O <sub>4</sub> Nanoparticles/Films Synthesized in a Vapor-Fed Flame Aerosol Reactor for Oxygen Evolution. ACS Applied Energy Materials, 2018, 1, 655-665.	5.1	20
30	A Highly Efficient Oxygen Evolution Catalyst Consisting of Interconnected Nickel–Iron‣ayered Double Hydroxide and Carbon Nanodomains. Advanced Materials, 2018, 30, 1705106.	21.0	209
31	Premixed Stagnation Flame Synthesized TiO <sub>2</sub> Nanoparticles with Mixed Phases for Efficient Photocatalytic Hydrogen Generation. ACS Sustainable Chemistry and Engineering, 2018, 6, 14470-14479.	6.7	25
32	Aminoâ€Assisted Anchoring of CsPbBr <sub>3</sub> Perovskite Quantum Dots on Porous gâ€C <sub>3</sub> N <sub>4</sub> for Enhanced Photocatalytic CO <sub>2</sub> Reduction. Angewandte Chemie, 2018, 130, 13758-13762.	2.0	172
33	Aminoâ€Assisted Anchoring of CsPbBr <sub>3</sub> Perovskite Quantum Dots on Porous g <sub>3</sub> N <sub>4</sub> for Enhanced Photocatalytic CO <sub>2</sub> Reduction. Angewandte Chemie - International Edition, 2018, 57, 13570-13574.	13.8	432
34	Rational Design of Catalytic Centers in Crystalline Frameworks. Advanced Materials, 2018, 30, e1707582.	21.0	103
35	Nickel Nanoparticles Encapsulated in Few‣ayer Nitrogenâ€Đoped Graphene Derived from Metal–Organic Frameworks as Efficient Bifunctional Electrocatalysts for Overall Water Splitting. Advanced Materials, 2017, 29, 1605957.	21.0	507
36	Crystalline In–Sb–S framework for highly-performed lithium/sodium storage. Journal of Materials Chemistry A, 2017, 5, 14198-14205.	10.3	20

#	Article	IF	CITATIONS
37	Self-template synthesis of CdS/NiS <sub>x</sub> heterostructured nanohybrids for efficient photocatalytic hydrogen evolution. Dalton Transactions, 2017, 46, 10650-10656.	3.3	25
38	Syntheses, crystal structures, and photocatalytic properties of two ammonium-directed Ag–Sb–S complexes. Inorganic Chemistry Frontiers, 2017, 4, 954-959.	6.0	26
39	Unique PCoN Surface Bonding States Constructed on g <sub>3</sub> N <sub>4</sub> Nanosheets for Drastically Enhanced Photocatalytic Activity of H <sub>2</sub> Evolution. Advanced Functional Materials, 2017, 27, 1604328.	14.9	329
40	Metal-free photocatalysts for various applications in energy conversion and environmental purification. Green Chemistry, 2017, 19, 882-899.	9.0	261
41	Evolution of hydrogen by few-layered black phosphorus under visible illumination. Journal of Materials Chemistry A, 2017, 5, 24874-24879.	10.3	45
42	Homoepitaxial growth on semiconductor nanocrystals for efficient and stable visible-light photocatalytic hydrogen evolution. Nanoscale, 2017, 9, 17794-17801.	5.6	11
43	A spongy nickel-organic CO <sub>2</sub> reduction photocatalyst for nearly 100% selective CO production. Science Advances, 2017, 3, e1700921.	10.3	175
44	Phosphonate-Based Metal–Organic Framework Derived Co–P–C Hybrid as an Efficient Electrocatalyst for Oxygen Evolution Reaction. ACS Catalysis, 2017, 7, 6000-6007.	11.2	149
45	CdS nanoparticles loaded on porous poly-melamine–formaldehyde polymer for photocatalytic dye degradation. Research on Chemical Intermediates, 2017, 43, 5083-5090.	2.7	8
46	Investigating the Role of Tunable Nitrogen Vacancies in Graphitic Carbon Nitride Nanosheets for Efficient Visible-Light-Driven H <sub>2</sub> Evolution and CO <sub>2</sub> Reduction. ACS Sustainable Chemistry and Engineering, 2017, 5, 7260-7268.	6.7	322
47	<i>In vivo </i> Biocompatibility, Biodistribution and Therapeutic Efficiency of Titania Coated Upconversion Nanoparticles for Photodynamic Therapy of Solid Oral Cancers. Theranostics, 2016, 6, 1844-1865.	10.0	92
48	Nitrogen-doped cobalt phosphate@nanocarbon hybrids for efficient electrocatalytic oxygen reduction. Energy and Environmental Science, 2016, 9, 2563-2570.	30.8	216
49	Metal-free carbonaceous electrocatalysts and photocatalysts for water splitting. Chemical Society Reviews, 2016, 45, 3039-3052.	38.1	499
50	A highly efficient noble metal free photocatalytic hydrogen evolution system containing MoP and CdS quantum dots. Nanoscale, 2016, 8, 14438-14447.	5.6	77
51	A surfactant-thermal method to prepare crystalline thioantimonate for high-performance lithium-ion batteries. Inorganic Chemistry Frontiers, 2016, 3, 111-116.	6.0	32
52	Single-layer MoS <sub>2</sub> nanosheet grafted upconversion nanoparticles for near-infrared fluorescence imaging-guided deep tissue cancer phototherapy. Nanoscale, 2016, 8, 7861-7865.	5.6	84
53	CdS quantum dots and tungsten carbide supported on anatase–rutile composite TiO <sub>2</sub> for highly efficient visible-light-driven photocatalytic H <sub>2</sub> evolution from water. Catalysis Science and Technology, 2016, 6, 2206-2213.	4.1	62
54	Fabrication of a catalytic polymer composite sheet enabling visible light-driven photocatalytic disinfection of water. Research on Chemical Intermediates, 2016, 42, 4827-4838.	2.7	1

#	Article	IF	CITATIONS
55	Nickel-based cocatalysts for photocatalytic hydrogen production. Applied Surface Science, 2015, 351, 779-793.	6.1	213
56	Recent progress in g-C <sub>3</sub> N <sub>4</sub> based low cost photocatalytic system: activity enhancement and emerging applications. Catalysis Science and Technology, 2015, 5, 5048-5061.	4.1	206
57	A crystalline Cu–Sn–S framework for high-performance lithium storage. Journal of Materials Chemistry A, 2015, 3, 19410-19416.	10.3	60
58	Oxygen permeation behavior through Ce <sub>0.9</sub> Gd <sub>0.1</sub> O <sub>2â´î´</sub> membranes electronically short-circuited by dual-phase Ce <sub>0.9</sub> Gd <sub>0.1</sub> O <sub>2â´î´</sub> –Ag decoration. Journal of Materials Chemistry A, 2015, 3, 19033-19041.	10.3	21
59	Metal–organic framework immobilized cobalt oxide nanoparticles for efficient photocatalytic water oxidation. Journal of Materials Chemistry A, 2015, 3, 20607-20613.	10.3	57
60	Bio-inspired organic cobalt( <scp>ii</scp> ) phosphonates toward water oxidation. Energy and Environmental Science, 2015, 8, 526-534.	30.8	79
61	Photocatalysis. Beilstein Journal of Nanotechnology, 2014, 5, 1071-1072.	2.8	2
62	Photocatalytic Reduction of Carbon Dioxide over Selfâ€Assembled Carbon Nitride and Layered Double Hydroxide: The Role of Carbon Dioxide Enrichment. ChemCatChem, 2014, 6, 2315-2321.	3.7	130
63	Surfactant-thermal method to prepare two novel two-dimensional Mn–Sb–S compounds for photocatalytic applications. Journal of Solid State Chemistry, 2014, 220, 118-123.	2.9	31
64	Development of high refractive ZnS/PVP/PDMAA hydrogel nanocomposites for artificial cornea implants. Acta Biomaterialia, 2014, 10, 1167-1176.	8.3	43
65	Effect of depositing silver nanoparticles on BiVO <sub>4</sub> in enhancing visible light photocatalytic inactivation of bacteria in water. Journal of Materials Chemistry A, 2014, 2, 6209-6217.	10.3	107
66	Post-synthesis modification of a metal–organic framework to construct a bifunctional photocatalyst for hydrogen production. Energy and Environmental Science, 2013, 6, 3229.	30.8	336
67	Development of optically transparent ZnS/poly(vinylpyrrolidone) nanocomposite films with high refractive indices and high Abbe numbers. Journal of Applied Polymer Science, 2013, 129, 1793-1798.	2.6	14
68	Immobilizing CdS quantum dots and dendritic Pt nanocrystals on thiolated graphene nanosheets toward highly efficient photocatalytic H2 evolution. Nanoscale, 2013, 5, 9830.	5.6	110
69	A facile synthesis of monodispersed hierarchical layered double hydroxide on silica spheres for efficient removal of pharmaceuticals from water. Journal of Materials Chemistry A, 2013, 1, 3877.	10.3	59
70	Porous Fe2O3 nanocubes derived from MOFs for highly reversible lithium storage. CrystEngComm, 2013, 15, 9332.	2.6	124
71	Photocatalytic reduction of CO2: a brief review on product analysis and systematic methods. Analytical Methods, 2013, 5, 1086.	2.7	186
72	Carbon nitride nanosheets for photocatalytic hydrogen evolution: remarkably enhanced activity by dye sensitization. Catalysis Science and Technology, 2013, 3, 1703.	4.1	225

#	Article	IF	CITATIONS
73	Photochemical Deposition of Pt on CdS for H <sub>2</sub> Evolution from Water: Markedly Enhanced Activity by Controlling Pt Reduction Environment. Journal of Physical Chemistry C, 2013, 117, 783-790.	3.1	178
74	Kinetically Controlling Phase Transformations of Crystalline Mercury Selenidostannates through Surfactant Media. Inorganic Chemistry, 2013, 52, 4148-4150.	4.0	121
75	Robust ion-transporting ceramic membrane with an internal short circuit for oxygen production. Journal of Materials Chemistry A, 2013, 1, 9150.	10.3	28
76	Formation of Sn@C Yolk–Shell Nanospheres and Core–Sheath Nanowires for Highly Reversible Lithium Storage. Particle and Particle Systems Characterization, 2013, 30, 873-880.	2.3	43
77	Nickel-complexes with a mixed-donor ligand for photocatalytic hydrogen evolution from aqueous solutions under visible light. RSC Advances, 2012, 2, 8293.	3.6	38
78	Formation of 1D Hierarchical Structures Composed of Ni <sub>3</sub> S <sub>2</sub> Nanosheets on CNTs Backbone for Supercapacitors and Photocatalytic H <sub>2</sub> Production. Advanced Energy Materials, 2012, 2, 1497-1502.	19.5	321
79	High Refractive Index Inorganic–Organic Interpenetrating Polymer Network (IPN) Hydrogel Nanocomposite toward Artificial Cornea Implants. ACS Macro Letters, 2012, 1, 876-881.	4.8	48
80	Ni <sup>2+</sup> -doped Zn <sub>x</sub> Cd <sub>1â^'x</sub> S photocatalysts from single-source precursors for efficient solar hydrogen production under visible light irradiation. Catalysis Science and Technology, 2012, 2, 581-588.	4.1	66
81	Mesoporous carbon nitride with in situ sulfur doping for enhanced photocatalytic hydrogen evolution from water under visible light. Journal of Materials Chemistry, 2012, 22, 15006.	6.7	632
82	Growth of Metal–Metal Oxide Nanostructures on Freestanding Graphene Paper for Flexible Biosensors. Advanced Functional Materials, 2012, 22, 2487-2494.	14.9	246
83	Cobalt Phosphate–ZnO Composite Photocatalysts for Oxygen Evolution from Photocatalytic Water Oxidation. Industrial & Engineering Chemistry Research, 2012, 51, 9945-9951.	3.7	71
84	Silver Nanoparticles Deposited Layered Double Hydroxide Nanoporous Coatings with Excellent Antimicrobial Activities. Advanced Functional Materials, 2012, 22, 780-787.	14.9	145
85	Highly active ZnxCd1â^'xS photocatalysts containing earth abundant elements only for H2 production from water under visible light. Catalysis Science and Technology, 2011, 1, 940.	4.1	80
86	Hybrid Functionals Study of Band Bowing, Band Edges and Electronic Structures of Cd <sub>1–<i>x</i></sub> Zn <sub><i>x</i></sub> S Solid Solution. Journal of Physical Chemistry C, 2011, 115, 19741-19748.	3.1	88
87	Self-assembled Fe <sub>3</sub> O <sub>4</sub> -layered double hydroxide colloidal nanohybrids with excellent performance for treatment of organic dyes in water. Journal of Materials Chemistry, 2011, 21, 1218-1225.	6.7	206
88	Effect of molecular weight and substrate on silicone segregation from UV resin at plasma polymerized mold interface. Journal of Polymer Science, Part B: Polymer Physics, 2010, 48, 442-450.	2.1	1
89	Highly efficient and noble metal-free NiS/CdS photocatalysts for H2 evolution from lactic acid sacrificial solution under visible light. Chemical Communications, 2010, 46, 7631.	4.1	450
90	The Origin of Visible Light Absorption in Chalcogen Element (S, Se, and Te)-Doped Anatase TiO <sub>2</sub> Photocatalysts. Journal of Physical Chemistry C, 2010, 114, 7063-7069.	3.1	61

#	Article	IF	CITATIONS
91	ZnO/ZnFe <sub>2</sub> O <sub>4</sub> Magnetic Fluorescent Bifunctional Hollow Nanospheres: Synthesis, Characterization, and Their Optical/Magnetic Properties. Journal of Physical Chemistry C, 2010, 114, 17455-17459.	3.1	58
92	Tb-doped iron oxide: bifunctional fluorescent and magnetic nanocrystals. Journal of Materials Chemistry, 2009, 19, 3696.	6.7	51
93	Direct Assembly of Anisotropic Layered Double Hydroxide (LDH) Nanocrystals on Spherical Template for Fabrication of Drug-LDH Hollow Nanospheres. Chemistry of Materials, 2009, 21, 781-783.	6.7	120
94	Template-Free Synthesis of Highly Uniform α-GaOOH Spindles and Conversion to α-Ga <sub>2</sub> O <sub>3</sub> and β-Ga <sub>2</sub> O <sub>3</sub> . Crystal Growth and Design, 2008, 8, 1282-1287.	3.0	80
95	Synthesis of unusual coral-like layered double hydroxide microspheres in a nonaqueous polar solvent/surfactant system. Journal of Materials Chemistry, 2008, 18, 2112.	6.7	64
96	Y2O3:Tb Nanocrystals Self-Assembly into Nanorods by Oriented Attachment Mechanism. Journal of Physical Chemistry C, 2007, 111, 7893-7897.	3.1	57
97	Report on the 4th Asia Pacific Congress on Catalysis (APCAT 4). Catalysis Surveys From Asia, 2007, 11, 192-193.	2.6	Ο